JACS JOURNAL OF THE AMERICAN CHEMICAL SOCIETY

Communication

Cite This: J. Am. Chem. Soc. 2019, 141, 18390−18394

pubs.acs.org/JACS

A Simple Molecular Design Strategy for Delayed Fluorescence toward 1000 nm

Daniel G. Congrave,*[,§,†] Bluebell H. Drummond,[§,‡] Patrick J. Conaghan,[‡] Haydn Francis,[†] Saul T. E. Jones,[‡] Clare P. Grey,[†] Neil C. Greenham,[‡] Dan Credgington,[‡] and Hugo Bronstein*[,†,‡]

[†]Department of Chemistry, University of Cambridge, Cambridge, CB2 1EW, U.K.

[‡]Cavendish Laboratory, University of Cambridge, Cambridge, CB3 0HE, U.K.

Supporting Information

ABSTRACT: Harnessing the near-infrared (NIR) region of the electromagnetic spectrum is exceedingly important for photovoltaics, telecommunications, and the biomedical sciences. While thermally activated delayed fluorescent (TADF) materials have attracted much interest due to their intense luminescence and narrow exchange energies (ΔE_{ST}), they are still greatly inferior to conventional fluorescent dyes in the NIR, which precludes their application. This is because securing a sufficiently strong donor−acceptor (D−A) interaction for NIR emission alongside the narrow ΔE_{ST} required for TADF is highly challenging. Here, we demonstrate that by abandoning the common polydonor model in favor of a D−A dyad structure, a sufficiently strong D−A interaction can be obtained to realize a TADF emitter capable of photoluminescence (PL) close to 1000 nm. Electroluminescence (EL) at a peak wavelength of 904 nm is also reported. This strategy is both conceptually and synthetically simple and offers a new approach to the development of future NIR TADF materials.

All-organic materials exhibiting thermally activated delayed fluorescence (TADF) have emerged as next generation dopants in organic light-emitting devices (OLEDs).[1,2] Efficient emission has been reported throughout the visible spectrum, facilitated by modular synthesis and rational design.[3] Despite this, it has not yet been possible to realize efficient emission in the near-infrared (NIR) region (ca. 700−1000 nm).[4−7] The longest wavelength TADF emitter reported to date exhibits a maximum peak emission wavelength (λ_{max}) of ca. 800 nm,[8] marginally outside the visible spectrum, and considerably below the values of ≥1000 nm that are well established for first generation fluorescent emitters.[5,7,9,10] Consequently, shifting the emission from TADF materials to comparably low energies remains an immediate challenge if potential applications in telecommunications, night vision, organic photovoltaic devices (OPVs), organic lasers, photodetectors, and NIR bioimaging are to be realized.[5,6,11]

All-organic TADF emitters are typically assembled from electron-rich donor (D) and electron-poor acceptor (A) heterocycles, with twisted linkages to ensure a small exchange energy (ΔE_{ST}). Emission occurs from an intramolecular charge transfer (ICT) state. Since the seminal structures reported by Adachi et al. (e.g., 4CzIPN),[12,13] there has been an overwhelming trend toward acceptor cores functionalized with multiple peripheral donors, i.e., polydonor D_n−A structures where $n > 1$.[2] This also applies to the vast majority of deep-red and NIR TADF candidates published to date.[6,14−21] For example, Jiang, Liao and co-workers reported a D_2−A acenaphthene-based emitter (**APDC-DTPA**) (Figure 1) which exhibits emission at λ_{max} = 687 nm and a photoluminescence quantum yield (PLQY) of 63% when doped into TBPi at 10 wt % (λ_{max} = 756 nm, PLQY = 17% in neat film).[15] Adachi et al. also studied two NIR TADF dyes based on unconventional boron curcuminoid acceptors.[8,16] The redder D_4−A_2 analogue (Figure 1) emits at λ_{max} = 801 nm with a PLQY of 4% at 40 wt % in CBP. These examples constitute the current state-of-the-art NIR TADF emitters.

An exceptionally stabilized ICT state is required for NIR TADF. This is intuitively achieved through ensuring the D−A interaction is as strong as possible, which is compromised in common polydonor designs. This is because the multiple peripheral donors that are typically employed in TADF materials are not directly electronically coupled, reducing their additive effect.[12,22,23] An increase in the number of donors, while enhancing the net donor strength, also suppresses the strength of the acceptor through functionalizing it with an increasing number of discrete electron-donating groups, compromising any red shift. For many red TADF materials,[19,22−25] any bathochromic shift in emission afforded by additional donors is incremental at best compared to single-donor D−A dyads, which now comprise a noteworthy portion of the most efficient red examples.[26,27] It was also recently demonstrated that converting D_2−A **APDC-DTPA** into its D−A analogue **TPAAP** (Figure 1) red-shifts the PL by 21 to 777 nm in a neat film (PLQY = 20%).[28] Herein, we demonstrate a simple concept to afford unprecedented progress into the NIR through adopting an uncomplicated D−A dyad structure.

The structure of the new NIR TADF emitter, **CAT-1**, is shown in Figures 1 and 2. It can be easily synthesized (Scheme S1) on a multigram scale for thermal evaporation (T_d = 409 °C, T_g = 128 °C) (Figure S3) with minimal chromatography. The removal of an electron donor in **APDC-DTPA** to afford **TPAAP** facilitates an incremental 21 nm red shift in neat film emission.[28] In **CAT-1** we take greater advantage of the D−A dyad structure by replacing the second electron donor with a

Received: August 28, 2019
Published: October 29, 2019

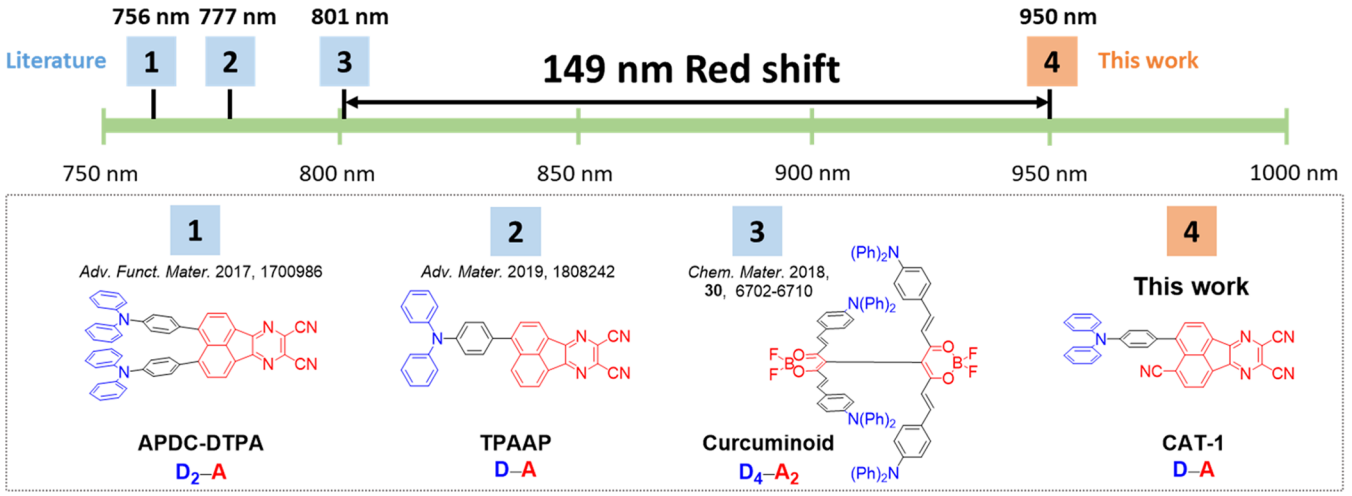

Figure 1. Molecular structures of **CAT-1** and state-of-the-art NIR TADF materials and their lowest-energy reported photoluminescence λ_{max} values.

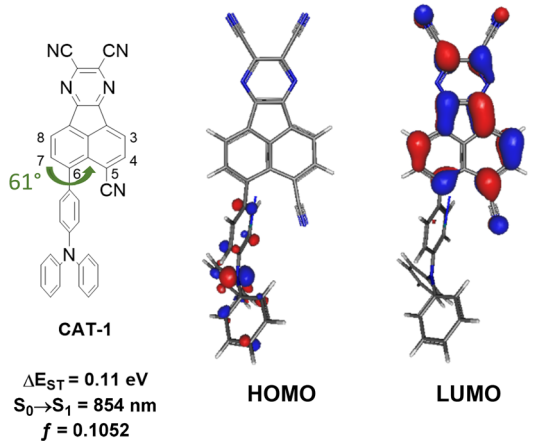

Figure 2. Numbering scheme, parameters calculated by TD-B3LYP/6-31G* and HOMO and LUMO distributions for **CAT-1**.

more beneficial electron-withdrawing CN group.[29−33] The additional CN group is both proximal to the single electron donor and directly conjugated to it via the pyrazine moiety, which may contribute to the greatly increased acceptor strength (Figure S1). This simple and rational addition substantially stabilizes ICT to obtain unprecedentedly red-shifted PL from a NIR TADF material.

CAT-1 was designed using DFT/TD-DFT (B3LYP/6-31G*) (Figure 2, Figure S4, Tables S2−S8). In the optimized geometry the phenyl spacer-acceptor dihedral angle of 61°, ensures a narrow calculated ΔE_{ST} of 0.11 eV. Nevertheless, an oscillator strength (f) of 0.1052 for the $S_0 \rightarrow S_1$ excitation is maintained (Table S3). This compares favorably with other NIR emitters that have narrow calculated ΔE_{ST} values[14,19,30] (e.g., **APDC-DTPA** (ΔE_{ST} = 0.10 eV, f = 0.0266; Table S4)).[15] We note that TD-PBE0/def2-SVP, TDA-PBE0/def2-SVP, and TDA-PBE0/def2-TZVP all also predict narrow ΔE_{ST} values ≤0.15 eV (Tables S6−S8).[34,35] Cyclic voltammetry (Figure S2, Table S1) indicates that the additional CN affords a deep[14,15,28,29] LUMO energy of −4.11 eV (HOMO = −5.64 eV) and a very narrow electrochemical band gap (1.53 eV), highlighting the high strength of the new electron acceptor unit.

The photophysical properties of **CAT-1** were studied in dilute solution, doped evaporated films (with CBP as host), and neat films prepared by both thermal evaporation and drop-casting. λ_{max} and PLQY data are summarized in Table 1 (further data are recorded in Table S10).

Table 1. Summary of the PL Data for CAT-1

sample preparation	λ_{max} PL/nm	PLQY[a] /%
toluene solution	770	3.9 ± 0.4
10 wt % in CBP	763	8.8 ± 0.2
40 wt % in CBP	820	1.98 ± 0.04
neat evaporated	887	0.18 ± 0.04
neat drop-cast	950	≤0.18

[a]Absolute PLQY measured using an integrating sphere.

The absorption spectrum in toluene consists of three major bands (Figure 3). The high energy region (≤380 nm) is ascribed to local $\pi-\pi^*$ transitions, the broad low energy band centered at 560 nm is assigned to D−A ICT, and the shoulder around 450 nm is mixed character. This assignment is supported by TD-DFT (Figure S7). The photoluminescence (PL) is broad and unstructured (toluene λ_{max} = 770 nm) and exhibits positive solvatochromism (Figures S10 and S11, Table S9), indicating emission from an ICT state. A large red shift in solution PL compared to **APDC-DTPA**[15] (130 nm) highlights the intrinsic efficacy of the design strategy in the absence of aggregation.

When doped into CBP at 10 wt %, **CAT-1** exhibits low-energy emission with λ_{max} = 763 nm and a PLQY of 8.8 ± 0.2% (Figure 3). As well as prompt fluorescence (τ < 5 ns), a delayed component (τ = 80 μs, 13.5% contribution) to the PL is also observed (Figure 3, Figure S13). The delayed PL is spectrally similar to the prompt (Figure S14) and is thus assigned to delayed fluorescence from the same state. The intensity of the delayed fluorescence increases with temperature between 10 and 292 K, confirming a TADF mechanism (Figure S17). It is also significantly quenched in the presence of oxygen (Figure S13), indicating a contribution from triplet states, as expected. Furthermore, a narrow ΔE_{ST} of ca. 0.04 eV was estimated experimentally from the onsets of the low temperature fluorescence and phosphorescence spectra of **CAT-1** in CBP at 10 wt % (Figure S19).

Increasing the doping ratio of **CAT-1** in the evaporated films leads to significant bathochromic shifts in emission (Figure 3,

DOI: 10.1021/jacs.9b09323
J. Am. Chem. Soc. 2019, 141, 18390−18394

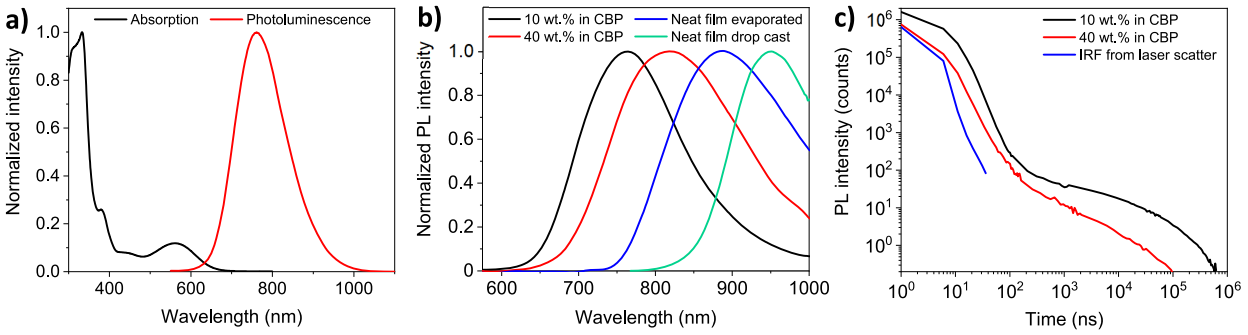

Figure 3. (a) Normalized absorption and PL spectra for **CAT-1** in toluene. λ_{ex} = 520 nm. (b) Normalized Steady state PL spectra for **CAT-1** in doped and neat films. λ_{ex} = 520 nm. Spectra are reported to 1000 nm due to the low detector sensitivity beyond 1000 nm. (c) Time-resolved PL intensity of **CAT-1** doped into CBP at different weight ratios recorded in 10^{-3} mbar vacuum. Instrument response function (IRF) plotted in blue. λ_{ex} = 400 nm.

Table 1, Table S10). This is common for highly polar TADF materials and is attributed to the effects of solvatochromism and aggregation.[7,28,36] This is also accompanied by a sequential decrease in PLQY,[16,28] indicating a trade-off between PL wavelength and quantum efficiency when exploiting aggregation to red-shift emission. When **CAT-1** is doped into CBP at 40 wt %, emission is recorded at λ_{max} = 820 nm with a TADF component still present (τ = 8 μs, 5.1% contribution) (Figures S13 and S18). This is lower in energy than for the D_4−A_2 curcuminoid derivative reported by Adachi et al. (λ_{max} = 801 nm) (Figure 1),[8] although our PLQY is lower (2% vs 4%). Unlike the curcuminoid the molecular weight of **CAT-1** is also sufficiently low for desirable thermal evaporation.[14,15,29] To the best of our knowledge this is the lowest-energy TADF confirmed by variable temperature time-resolved measurements to date (Table S11).

In evaporated films of **CAT-1** PL is recorded with λ_{max} = 887 nm (Figure 3). While the signal-to-noise ratio is poor due to the low PLQY, the longer lifetime component of the PL decay also appears to be quenched in the presence of oxygen (Figures S15 and S16). Emission from films drop-cast from chlorobenzene solution is further reproducibly red-shifted to λ_{max} = 950 nm with a sharpening of the onset (Figure 3) and an associated red shift of the absorption spectrum (Figure S9). A similar PL red shift upon solution processing was recently reported for a red TADF emitter.[21,37] Analysis of the drop-cast film by thin film X-ray diffraction indicates a degree of solid state ordering consistent with enhanced aggregation (Figures S26 and S27). The large PL red shift in the drop-cast films is attributed to this.[28] No such crystallinity could be observed for the evaporated film, although this may be related to the low film thickness (Figure S28). While reabsorption in the comparatively thick drop-cast films may also influence this red shift in PL, such a dependence of the emission color on the processing method (e.g., thermal evaporation or solution processing) is well recognized for TADF materials.[38−41]

In summary, strategic replacement of the second electron donor of **APDC-DTPA** with a CN group in **CAT-1** affords large bathochromic shifts in PL: 130 nm in toluene, 76 nm in 10 wt % doped film, and 131 nm in evaporated film. This is considerably greater than the evaporated film red shift of 21 nm obtained upon sole removal of an electron donor (**TPAAP**) (Figure S20).[15,28] Notably, when doped into CBP at 10 wt % **CAT-1** also emits with a longer wavelength PL λ_{max} (763 nm) than **APDC-DTPA** in a neat evaporated film (756 nm). While the low PLQY precludes unambiguous confirmation of TADF in the drop-cast film, the PL λ_{max} of 950 nm is red-shifted by 149 nm compared to the longest wavelength PL λ_{max} reported thus far for a TADF-capable emitter (curcuminoid, Figure 1, Table S11).[8] Furthermore, **CAT-1** can display an emission spectrum for which the entirety of the PL falls >700 nm, which is considered "real" NIR.[7,11] In fact, the drop-cast film has an impressive PL onset of ca. 800 nm, which is exceptional for a material capable of TADF.[11]

The electroluminescence (EL) performance of **CAT-1** was also evaluated in preliminary thermally evaporated OLED devices (Figures S21−S25). Crucially, we note that undoped devices exhibit complete NIR (>700 nm) emission with an EL λ_{max} of 904 nm (Figure 4). This red shift in the undoped EL

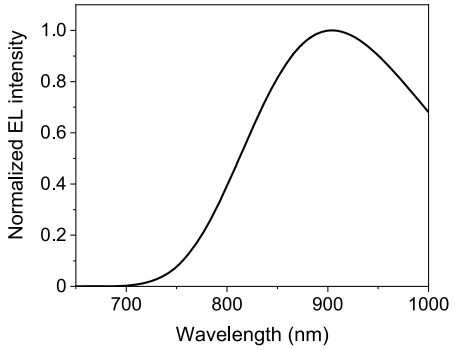

Figure 4. EL spectrum for an undoped **CAT-1** OLED at 5 V. λ_{max} = 904 nm.

compared to the neat evaporated film PL (904 nm vs 887 nm) may be because excitons are formed via a diffusional process in the device rather than direct photoexcitation. Optical interference is another possible explanation. While the maximum external quantum efficiency (ca. 0.019%) and radiance (ca. 1 × 10^3 mW sr^{-1} m^{-2}) are low, the peak EL λ_{max} is much lower in energy than for any previously reported TADF material (>100 nm), while being competitive with conventional fluorescent devices and red-shifted compared to almost all phosphorescent examples.[11] These data importantly confirm that the favorable long-wavelength PL of a neat film of **CAT-1** can be retained in an EL device.

In conclusion, this work provides a great advance into the NIR from a delayed fluorescent material. At the high donor and acceptor strengths required for NIR TADF, the incorporation of multiple donors is essentially ineffectual at red-shifting emission.[19,22−25,28] In contrast we have shown that

DOI: 10.1021/jacs.9b09323
J. Am. Chem. Soc. 2019, 141, 18390−18394

adopting an intrinsically simple D−A system structurally liberates molecules for rational functionalization to greatly stabilize the ICT state. We have succeeded in obtaining a dramatic red shift in PL λ_{max} of over 100 nm from a material capable of TADF compared to previous work (Figure 1). This facilitated fabrication of OLEDs displaying impressive EL λ_{max} values of >900 nm. The next step is clearly to improve the PLQY in this newly accessed low-energy region. This may be possible through incorporation of a more rigid electron donor capable of suppressing aggregation-induced quenching. Nevertheless, with respect to emission wavelength, **CAT-1** affords rapid and important progress. These unprecedented results crucially stem from a design strategy that is conceptually simple and easy to implement synthetically. It will be broadly applicable to other systems and heavily influence future NIR TADF design.

■ ASSOCIATED CONTENT

Supporting Information

The Supporting Information is available free of charge on the ACS Publications website at DOI: 10.1021/jacs.9b09323.

NMR spectra, electrochemical data, thermogravimetric analysis, computational data, additional photophysical and device data, and thin film X-ray diffraction data (PDF)

■ AUTHOR INFORMATION

Corresponding Authors

*dc704@cam.ac.uk
*hab60@cam.ac.uk

ORCID

Bluebell H. Drummond: 0000-0001-5940-8631
Saul T. E. Jones: 0000-0001-6007-2530
Clare P. Grey: 0000-0001-5572-192X
Neil C. Greenham: 0000-0002-2155-2432
Hugo Bronstein: 0000-0003-0293-8775

Author Contributions

§D.G.C. and B.H.D. contributed equally.

Notes

The authors declare no competing financial interest.

■ ACKNOWLEDGMENTS

Prof. Martin R. Bryce is aknowledged for use of his potentiostat at Durham University UK. This work was supported by the Engineering and Physical Sciences Research Council (Grant Nos. EP/M005143/1 and EP/S003126/1) and the European Research Council (ERC). D.C. and S.T.E.J. acknowledge support from the Royal Society (Grant Nos. UF130278 and RG140472). B.H.D. acknowledges support from the EPSRC Cambridge NanoDTC (Grant No. EP/L015978/1).

■ REFERENCES

(1) Liu, Y.; Li, C.; Ren, Z.; Yan, S.; Bryce, M. R. All-Organic Thermally Activated Delayed Fluorescence Materials for Organic Light-Emitting Diodes. *Nat. Rev. Mater.* **2018**, *3*, 18020.

(2) Wong, M. Y.; Zysman-Colman, E. Purely Organic Thermally Activated Delayed Fluorescence Materials for Organic Light-Emitting Diodes. *Adv. Mater.* **2017**, *29*, 1605444.

(3) Yang, Z.; Mao, Z.; Xie, Z.; Zhang, Y.; Liu, S.; Zhao, J.; Xu, J.; Chi, Z.; Aldred, M. P. Recent Advances in Organic Thermally Activated Delayed Fluorescence Materials. *Chem. Soc. Rev.* **2017**, *46*, 915−1016.

(4) Ai, X.; Evans, E. W.; Dong, S.; Gillett, A. J.; Guo, H.; Chen, Y.; Hele, T. J. H.; Friend, R. H.; Li, F. Efficient Radical-Based Light-Emitting Diodes with Doublet Emission. *Nature* **2018**, *563*, 536−540.

(5) Lei, Z.; Sun, C.; Pei, P.; Wang, S.; Li, D.; Zhang, X.; Zhang, F. Stable, Wavelength-Tunable Fluorescent Dyes in the NIR-II Region for in-Vivo High-Contrast Bioimaging and Multiplexed Biosensing. *Angew. Chem., Int. Ed.* **2019**, *58*, 8166−8171.

(6) Kim, J. H.; Yun, J. H.; Lee, J. Y. Recent Progress of Highly Efficient Red and Near-Infrared Thermally Activated Delayed Fluorescent Emitters. *Adv. Opt. Mater.* **2018**, *6*, 1800255.

(7) Jiang, J.; Xu, Z.; Zhou, J.; Hanif, M.; Jiang, Q.; Hu, D.; Zhao, R.; Wang, C.; Liu, L.; Cao, Y. Enhanced Pi Conjugation and Donor/Acceptor Interactions in D - A - D Type Emitter for Highly E Ffi Cient Near-Infrared Organic Light- Emitting Diodes with an Emission Peak at 840 nm. *Chem. Mater.* **2019**, *31*, 6499−6505.

(8) Ye, H.; Kim, D. H.; Chen, X.; Sandanayaka, A. D. S.; Kim, J. U.; Zaborova, E.; Canard, G.; Tsuchiya, Y.; Choi, E. Y.; Wu, J. W.; Fages, F.; Bredas, J.-L.; D'Aléo, A.; Ribierre, J.-C.; Adachi, C. Near-Infrared Electroluminescence and Low Threshold Amplified Spontaneous Emission above 800 nm from a Thermally Activated Delayed Fluorescent Emitter. *Chem. Mater.* **2018**, *30*, 6702−6710.

(9) Qian, B. G.; Zhong, Z.; Luo, M.; Yu, D.; Zhang, Z.; Wang, Z. Y.; Ma, D. Simple and Efficient Near-Infrared Organic Chromophores for Light-Emitting Diodes with Single Electroluminescent Emission above 1000 nm. *Adv. Mater.* **2009**, *21*, 111−116.

(10) Qian, G.; Dai, B.; Luo, M.; Yu, D.; Zhan, J.; Zhang, Z.; Dongge, M.; Wang, Z. Y. Band Gap Tunable, Donor-Acceptor-Donor Charge-Transfer Heteroquinoid-Based Chromophores: Near Infrared Photoluminescence and Electroluminescence. *Chem. Mater.* **2008**, *20*, 6208−6216.

(11) Zampetti, A.; Minotto, A.; Cacialli, F. Near-Infrared (NIR) Organic Light-Emitting Diodes (OLEDs): Challenges and Opportunities. *Adv. Funct. Mater.* **2019**, *29*, 1807623.

(12) Uoyama, H.; Goushi, K.; Shizu, K.; Nomura, H.; Adachi, C. Highly Efficient Organic Light-Emitting Diodes from Delayed Fluorescence. *Nature* **2012**, *492*, 234−238.

(13) Endo, A.; Sato, K.; Yoshimura, K.; Kai, T.; Kawada, A.; Miyazaki, H.; Adachi, C. Efficient up-Conversion of Triplet Excitons into a Singlet State and Its Application for Organic Light Emitting Diodes. *Appl. Phys. Lett.* **2011**, *98*, 83302.

(14) Wang, S.; Yan, X.; Cheng, Z.; Zhang, H.; Liu, Y.; Wang, Y. Highly Efficient Near-Infrared Delayed Fluorescence Organic Light Emitting Diodes Using a Phenanthrene-Based Charge-Transfer Compound. *Angew. Chem., Int. Ed.* **2015**, *54*, 13068−13072.

(15) Yuan, Y.; Hu, Y.; Zhang, Y. X.; Lin, J. D.; Wang, Y. K.; Jiang, Z. Q.; Liao, L. S.; Lee, S. T. Over 10% EQE Near-Infrared Electroluminescence Based on a Thermally Activated Delayed Fluorescence Emitter. *Adv. Funct. Mater.* **2017**, *27*, 1700986.

(16) Kim, D.-H.; D'Aléo, A.; Chen, X.-K.; Sandanayaka, A. D. S.; Yao, D.; Zhao, L.; Komino, T.; Zaborova, E.; Canard, G.; Tsuchiya, Y.; Choi, E.; Wu, J. W.; Fages, F.; Brédas, J.-L.; Ribierre, J.-C.; Adachi, C. High-Efficiency Electroluminescence and Amplified Spontaneous Emission from a Thermally Activated Delayed Fluorescent Near-Infrared Emitter. *Nat. Photonics* **2018**, *12*, 98−104.

(17) Sun, K.; Chu, D.; Cui, Y.; Tian, W.; Sun, Y.; Jiang, W. Near-Infrared Thermally Activated Delayed Fluorescent Dendrimers for the Efficient Non-Doped Solution-Processed Organic Light-Emitting Diodes. *Org. Electron.* **2017**, *48*, 389−396.

(18) Ni, F.; Wu, Z.; Zhu, Z.; Chen, T.; Wu, K.; Zhong, C.; An, K.; Wei, D.; Ma, D.; Yang, C. Teaching an Old Acceptor New Tricks: Rationally Employing 2,1,3-Benzothiadiazole as Input to Design a Highly Efficient Red Thermally Activated Delayed Fluorescence Emitter. *J. Mater. Chem. C* **2017**, *5*, 1363−1368.

(19) Zhang, Q.; Kuwabara, H.; Potscavage, W. J.; Huang, S.; Hatae, Y.; Shibata, T.; Adachi, C. Anthraquinone-Based Intramolecular Charge-Transfer Compounds: Computational Molecular Design,

DOI: 10.1021/jacs.9b09323
J. Am. Chem. Soc. 2019, 141, 18390−18394

Thermally Activated Delayed Fluorescence, and Highly Efficient Red Electroluminescence. *J. Am. Chem. Soc.* **2014**, *136*, 18070−18081.
(20) Wang, S.; Cheng, Z.; Song, X.; Yan, X.; Ye, K.; Liu, Y.; Yang, G.; Wang, Y. Highly Efficient Long-Wavelength Thermally Activated Delayed Fluorescence OLEDs Based on Dicyanopyrazino Phenanthrene Derivatives. *ACS Appl. Mater. Interfaces* **2017**, *9*, 9892−9901.
(21) Chen, J.-X.; Tao, W.-W.; Xiao, Y.-F.; Wang, K.; Zhang, M.; Fan, X.-C.; Chen, W.-C.; Yu, J.; Li, S.; Geng, F.-X.; Zhang, X.; Lee, C.-S. Efficient Orange-Red Thermally Activated Delayed Fluorescence Emitters Feasible for Both Thermal Evaporation and Solution Process. *ACS Appl. Mater. Interfaces* **2019**, *11*, 29086−29093.
(22) Yu, L.; Wu, Z.; Xie, G.; Zeng, W.; Ma, D.; Yang, C. Molecular Design to Regulate the Photophysical Properties of Multifunctional TADF Emitters towards High-Performance TADF-Based OLEDs with EQEs up to 22.4% and Small Efficiency Roll-Offs. *Chem. Sci.* **2018**, *9*, 1385−1391.
(23) Tanaka, H.; Shizu, K.; Nakanotani, H.; Adachi, C. Twisted Intramolecular Charge Transfer State for Long-Wavelength Thermally Activated Delayed Fluorescence. *Chem. Mater.* **2013**, *25*, 3766−3771.
(24) Wei, X.; Bu, L.; Li, X.; Ågren, H.; Xie, Y. Full Color Emissions Based on Intramolecular Charge Transfer Effect Modulated by Formyl and Boron-Dipyrromethene Moieties. *Dyes Pigm.* **2017**, *136*, 480−487.
(25) Huang, B.; Ji, Y.; Li, Z.; Zhou, N.; Jiang, W.; Feng, Y.; Lin, B. Simple Aggregation − Induced Delayed Fluorescence Materials Based on Anthraquinone Derivatives for Highly Efficient Solution − Processed Red OLEDs. *J. Lumin.* **2017**, *187*, 414−420.
(26) Chen, J.-X.; Tao, W.-W.; Chen, W.-C.; Xiao, Y.-F.; Wang, K.; Cao, C.; Yu, J.; Li, S.; Geng, F.-X.; Adachi, C.; Lee, C.-S.; Zhang, X.-H. Red/Near-Infrared Thermally Activated Delayed Fluorescence OLEDs with Near 100% Internal Quantum Efficiency. *Angew. Chem., Int. Ed.* **2019**, *58*, 14660−14665.
(27) Zeng, W.; Zhou, T.; Ning, W.; Zhong, C.; He, J.; Gong, S.; Xie, G.; Yang, C. Realizing 22.5% External Quantum Efficiency for Solution-Processed Thermally Activated Delayed-Fluorescence OLEDs with Red Emission at 622 nm via a Synergistic Strategy of Molecular Engineering and Host Selection. *Adv. Mater.* **2019**, *31*, 1901404.
(28) Xue, J.; Liang, Q.; Wang, R.; Hou, J.; Li, W.; Peng, Q.; Shuai, Z.; Qiao, J. Highly Efficient Thermally Activated Delayed Fluorescence via J-Aggregates with Strong Intermolecular Charge Transfer. *Adv. Mater.* **2019**, *31*, 1808242.
(29) Li, C.; Duan, R.; Liang, B.; Han, G.; Wang, S.; Ye, K.; Liu, Y.; Yi, Y.; Wang, Y. Deep-Red to Near-Infrared Thermally Activated Delayed Fluorescence in Organic Solid Films and Electroluminescent Devices. *Angew. Chem., Int. Ed.* **2017**, *56*, 11525−11529.
(30) Furue, R.; Matsuo, K.; Ashikari, Y.; Ooka, H.; Amanokura, N.; Yasuda, T. Highly Efficient Red−Orange Delayed Fluorescence Emitters Based on Strong π-Accepting Dibenzophenazine and Dibenzoquinoxaline Cores: Toward a Rational Pure-Red OLED Design. *Adv. Opt. Mater.* **2018**, *6*, 1701147.
(31) Liu, Y.; Huang, H.; Zhou, T.; Wu, K.; Zhu, M.; Yu, J.; Xie, G.; Yang, C. Boosting Photoluminescence Quantum Yields of Triarylboron/phenoxazine Hybrids via Incorporation of Cyano Groups and Their Applications as TADF Emitters for High- Performance Solution-Processed OLEDs. *J. Mater. Chem. C* **2019**, *7*, 4778−4783.
(32) Lee, H. L.; Lee, K. H.; Lee, J. Y.; Hong, W. P. Management of Thermally Activated Delayed Fluorescence Using a Secondary Electron Accepting Unit in Thermally Activated Delayed Fluorescent Emitters. *J. Mater. Chem. C* **2019**, *7*, 6465−6474.
(33) Zhao, B.; Xie, G.; Wang, H.; Han, C.; Xu, H. Simply Structured Near-Infrared Emitters with a Multicyano Linear Acceptor for Solution-Processed Organic Light-Emitting Diodes. *Chem. - Eur. J.* **2019**, *25*, 1010−1017.
(34) Moral, M.; Muccioli, L.; Son, W.; Olivier, Y.; Sancho-Garcia, J. C. Theoretical Rationalization of the Singlet − Triplet Gap in OLEDs Materials : Impact of Charge-Transfer Character. *J. Chem. Theory Comput.* **2015**, *11*, 168−177.
(35) Zeng, W.; Gong, S.; Zhong, C.; Yang, C. Prediction of Oscillator Strength and Transition Dipole Moments with the Nuclear Ensemble Approach for Thermally Activated Delayed Fluorescence Emitters. *J. Phys. Chem. C* **2019**, *123*, 10081−10086.
(36) dos Santos, P. L.; Ward, J. S.; Congrave, D. G.; Batsanov, A. S.; Stacey, J. E.; Penfold, T. J.; Monkman, A. P.; Bryce, M. R. Triazatruxene: A Rigid Central Donor Unit for a D-A3 Thermally Activated Delayed Fluorescence Material Exhibiting Sub-Microsecond Reverse Intersystem Crossing and Unity Quantum Yield via Multiple Singlet-Triplet State Pairs. *Adv. Sci.* **2018**, *5*, 1700989.
(37) Cho, Y. J.; Aziz, H. Root Causes of the Limited Electroluminescence Stability of Organic Light-Emitting Devices Made by Solution-Coating. *ACS Appl. Mater. Interfaces* **2018**, *10*, 18113−18122.
(38) Xie, G.; Li, X.; Chen, D.; Wang, Z.; Cai, X.; Chen, D.; Li, Y.; Liu, K.; Cao, Y.; Su, S. J. Evaporation- and Solution-Process-Feasible Highly Efficient Thianthrene-9,9′,10,10′-Tetraoxide-Based Thermally Activated Delayed Fluorescence Emitters with Reduced Efficiency Roll-Off. *Adv. Mater.* **2016**, *28*, 181−187.
(39) Data, P.; Okazaki, M.; Minakata, S.; Takeda, Y. Thermally Activated Delayed Fluorescence: Vs. Room Temperature Phosphorescence by Conformation Control of Organic Single Molecules. *J. Mater. Chem. C* **2019**, *7*, 6616−6621.
(40) Data, P.; Takeda, Y. Recent Advancements in and the Future of Organic Emitters: TADF- and RTP-Active Multifunctional Organic Materials. *Chem. - Asian J.* **2019**, *14*, 1613−1636.
(41) Tsujimoto, H.; Ha, D. G.; Markopoulos, G.; Chae, H. S.; Baldo, M. A.; Swager, T. M. Thermally Activated Delayed Fluorescence and Aggregation Induced Emission with Through-Space Charge Transfer. *J. Am. Chem. Soc.* **2017**, *139*, 4894−4900.

DOI: 10.1021/jacs.9b09323
J. Am. Chem. Soc. 2019, 141, 18390−18394